



1 **Revisiting and attributing the global controls on terrestrial**
2 **ecosystem functions of climate and plant traits at FLUXNET**
3 **sites with causal networks**

4 Haiyang Shi^{1,2,4,5}, Geping Luo^{1,2,3,5}, Olaf Hellwich⁶, Alishir Kurban^{1,2,3,5}, Philippe De Maeyer^{1,2,4,5} and Tim Van
5 de Voorde^{4,5}

6

7 ¹ State Key Laboratory of Desert and Oasis Ecology, Xinjiang Institute of Ecology and Geography, Chinese
8 Academy of Sciences, Urumqi, Xinjiang, 830011, China.

9 ² College of Resources and Environment, University of the Chinese Academy of Sciences, 19 (A) Yuquan Road,
10 Beijing, 100049, China.

11 ³ Research Centre for Ecology and Environment of Central Asia, Chinese Academy of Sciences, Urumqi, China.

12 ⁴ Department of Geography, Ghent University, Ghent 9000, Belgium.

13 ⁵ Sino-Belgian Joint Laboratory of Geo-Information, Ghent, Belgium.

14 ⁶ Department of Computer Vision & Remote Sensing, Technische Universität Berlin, 10587 Berlin, Germany.

15

16 **Correspondence to:** Geping Luo (luogp@ms.xjb.ac.cn) and Olaf Hellwich (olaf.hellwich@tu-berlin.de)

17 **Submitted to:** *Biogeosciences*

18



19 **Abstract**

20 Using statistical methods that do not emphasize the systematic causality to attribute climate and plant traits to
21 control ecosystem function may produce biased perceptions. We revisit this issue using a Bayesian network
22 (BN) capable of quantifying causality. Based on expert knowledge and climate, vegetation, and ecosystem
23 function data from the FLUXNET flux stations, we constructed a BN containing the causal relationship of
24 'climate-plant trait-ecosystem function'. Based on the sensitivity analysis function of the BN, we attributed the
25 control of climate and plant traits to ecosystem function and compared the results with those based on Random
26 forests and correlation analysis. The main conclusions of this study include: BN can be used for the
27 quantification of causal relationships between complex ecosystems and climatic and environmental systems, and
28 enables the analysis of indirect effects among variables. The control of ecosystem function by climate variables
29 (especially mean temperature and mean vapor pressure deficit) may have been underestimated previously, and
30 the mechanism of indirect effects of climate variables on ecosystem function through plant traits should be
31 emphasized in future studies. Further inclusion of temporal information in BN holds promise for improving the
32 analysis of lagged effects and interactions and feedback effects between variables.

33 **1 Introduction**

34 Terrestrial ecosystems provide a variety of important ecosystem functions for our society (Manning et al.,
35 2018). It is essential to understand the potential changes in ecosystem functions in the context of global climate
36 change (Grimm et al., 2013). The response of terrestrial ecosystem function to changes in climate change, plant
37 traits, and environmental conditions, and the corresponding mechanisms, are complex due to enormous spatial
38 and temporal variations across ecosystems, climate zones, and also space-time scales (Diaz and Cabido, 1997;
39 Madani et al., 2018; Myers-Smith et al., 2019). Given the enormous variations, on the global scale, these issues
40 have not been clarified well.

41
42 In the past decades, measurements of ecosystem functions are increasingly available to support studies of the
43 relations between ecosystem functions and climate and environmental systems. For example, eddy-covariance
44 flux tower observations (Baldocchi, 2014) for carbon flux (i.e., net ecosystem exchange (NEE)) and water flux
45 (i.e., evapotranspiration (ET)) have been widely used to investigate changes in ecosystem functions and their
46 responses to climate change, vegetation condition changes, etc (Jung et al., 2020, 2010; Migliavacca et al., 2021;
47 Peaucelle et al., 2019). With the increase in such observations, various statistical analysis methods such as
48 emerging machine learning (Barnes et al., 2021; Migliavacca et al., 2021; Reichstein et al., 2019; Shi et al.,
49 2022b, a, 2020b; Tramontana et al., 2016) have been used to mine the hidden information on the effects of
50 climate change and its induced changes in vegetation, etc. on ecosystem function variables such as carbon and
51 water flux, which has not been understood in depth by process-based models (e.g., biogeochemistry models
52 (Sakschewski et al., 2016)). For example, using Random forests (RF) and principal component analysis (PCA),
53 a recent study (Migliavacca et al., 2021) quantified the three main axes of terrestrial ecosystem function and
54 their drivers based on observations of carbon and water fluxes of FLUXNET (Pastorello et al., 2020) and
55 various climate and plant trait variables. Generally, data-driven approaches have become increasingly important
56 recently in this area (Reichstein et al., 2019).



57

58 However, compared to the process-based models, most of these data-driven approaches lack representation of
59 the systematic causality and detailed processes in the relations between ecosystem function and climate and
60 environments, despite the widely recognized complex causal interactions of ecosystems with climate and
61 environmental systems (Reichstein et al., 2014). Conventional methods such as multiple linear regression have
62 been questioned in attribution studies of the relationship between climate and the carbon cycle (Wang et al.,
63 2022). For example, the use of multiple linear regression may underestimate the direct effect of soil moisture
64 possibly due to the covariance between variables (Wang et al., 2022). For machine learning techniques, although
65 current common algorithms such as RF (Migliavacca et al., 2021) can report the importance of features (IMP) to
66 measure their contributions to the prediction model, IMP-based attribution to the target variable can also be
67 unreliable when we aim to explain systematic causality (Gregorutti et al., 2017). Therefore, it is commonly
68 important to recognize the difference between correlation and causality in these approaches and emphasize the
69 systematic causality in the systems and also detailed causal relations between features in a data-driven approach.

70

71 Bayesian network (BN) is a causal model based on conditional probability representation (Friedman et al., 1997;
72 Pearl, 1985) that characterizes the transmission of cause and effect through conditional probabilities between
73 variables. Currently, BN has been used in modeling causal relationships in many fields and has demonstrated
74 advantages in causal interpretation, including in the fields such as hydrology and ecology (Chan et al., 2010;
75 Keshkar et al., 2013; Milns et al., 2010; Pollino et al., 2007; Shi et al., 2021a, b; Trifonova et al., 2015).
76 However, BN has rarely been used in the study of attribution of changes in ecosystem function. Therefore, this
77 study used BN to attribute the controls of climate and plant traits on ecosystem function by quantifying the
78 causal relationships involved. The data used are from a previous study (Migliavacca et al., 2021) which
79 extracted ecosystem function, climate, and plant trait variables for FLUXNET flux stations. The construction of
80 the causal structure of BN referred to the previous expert knowledge of this system (Reichstein et al., 2014).
81 Further, by comparing BN-based attribution analysis, linear correlation analysis, and RF-based IMP reported by
82 the previous study (Migliavacca et al., 2021), we investigated the adding-values of using BN for causal analysis
83 and discussed its prospects in this paper.

84 **2 Methodology**

85 **2.1 Data**

86 The used variables (Table 1) include the carbon and water fluxes of the FLUXNET flux tower sites and the
87 ecosystem function variables derived from them, and information on the corresponding climatic variables as
88 well as plant traits:

- 89 a) Ecosystem function variables: underlying Water Use Efficiency (uWUE), maximum evapotranspiration
90 (ETmax), maximum surface conductance (GSmax), maximum net CO₂ uptake of the ecosystem
91 (NEPmax), Gross Primary Productivity at light saturation (GPPsat), Mean basal ecosystem respiration at a
92 reference temperature of 15 °C (Rb).
- 93 b) Plant trait variables: ecosystem scale foliar nitrogen concentration (Nmass), Maximum Leaf Area Index
94 (LAI_{max}), Maximum vegetation height (Hc), Aboveground Biomass (AGB).



95 c) Mean incoming shortwave radiation (SWin), Mean temperature (Tair), Mean Vapor Pressure Deficit
 96 (VPD), Mean annual precipitation (P), and cumulative soil water index (CSWI).
 97
 98 These data have different producing processes, including those calculated from flux data, site records, extracted
 99 from remote sensing data, etc. The specific calculation methods can be found in the previous study (Migliavacca
 100 et al., 2021).

102 Table 1. The variables used and the discretization of their values in BN.

Variable node	Definition and units	Type	Approach (Migliavacca et al., 2021)	Discretization in BN (thresholds for classifications)
uWUE	underlying Water Use Efficiency [gC kPa ^{0.5} kgH ₂ O ⁻¹]	Ecosystem function	calculated from GPP, VPD, ET	0.0, 2.5, 3.5, 5.5
ETmax	maximum evapotranspiration in the growing season [mm]	Ecosystem function	computed as the 95th percentile of ET in the growing season	0.05, 0.15, 0.30, 0.45
GSmax	maximum surface conductance [m s ⁻¹]	Ecosystem function	computed by inverting the Penman-Monteith equation after calculating the aerodynamic conductance	0, 0.01, 0.02, 0.06
NEPmax	maximum net CO ₂ uptake of the ecosystem [umol CO ₂ m ⁻² s ⁻¹]	Ecosystem function	computed as the 90th percentile of the half-hourly net ecosystem production in the growing season	0, 15, 30, 45
GPPsat	Gross Primary Productivity at light saturation [umol CO ₂ m ⁻² s ⁻¹]	Ecosystem function	computed as the 90th percentile estimated from half-hourly data by fitting the hyperbolic light response curves	0, 15, 30, 50
Rb	Mean basal ecosystem respiration at a reference temperature of 15 °C [umol CO ₂ m ⁻² s ⁻¹]	Ecosystem function	derived from night-time NEE measurements	0, 2, 4, 12
Nmass	ecosystem scale foliar nitrogen concentration [gN 100 g ⁻¹]	Plant trait	computed as the community weighted average of foliar N% of the major species at the site sampled at the peak of the growing season or gathered	0.5, 1.25, 2.0, 4.5



			from the literature (Musavi et al., 2016, 2015; Fleischer et al., 2015; Flechard et al., 2020)	
LAImax	Maximum Leaf Area Index [m ² m ⁻²]	Plant trait	collected from the literature (Migliavacca et al., 2011; Flechard et al., 2020), the FLUXNET Biological Ancillary Data Management (BADM) product, and/or site principal investigators	0, 3, 6, 13
Hc	Maximum vegetation height [m]	Plant trait	collected from the literature (Migliavacca et al., 2011; Flechard et al., 2020), the BADM product, and/or site principal investigators	0, 5, 20, 80
AGB	Aboveground Biomass derived from the Globbiomass project [t DM ha ⁻¹]	Plant trait	extracted from the satellite-based GlobBiomass dataset (Santoro et al., 2021)	0, 50, 150, 350
SWin	Mean incoming shortwave radiation [W m ⁻²]	Climate	from FLUXNET data	50, 125, 200, 275
Tair	Mean temperature [degree C]	Climate	from FLUXNET data	-12, 5, 15, 30
VPD	Mean Vapor Pressure Deficit [hPa]	Climate	from FLUXNET data	0, 4, 8, 27
P	Mean annual precipitation [cm/year]	Climate	from FLUXNET data	0, 40, 80, 260
CSWI	cumulative soil water index	Climate-related soil water availability	computed as a measure of water availability (Nelson et al., 2018)	-100, -20, 0, 5

103

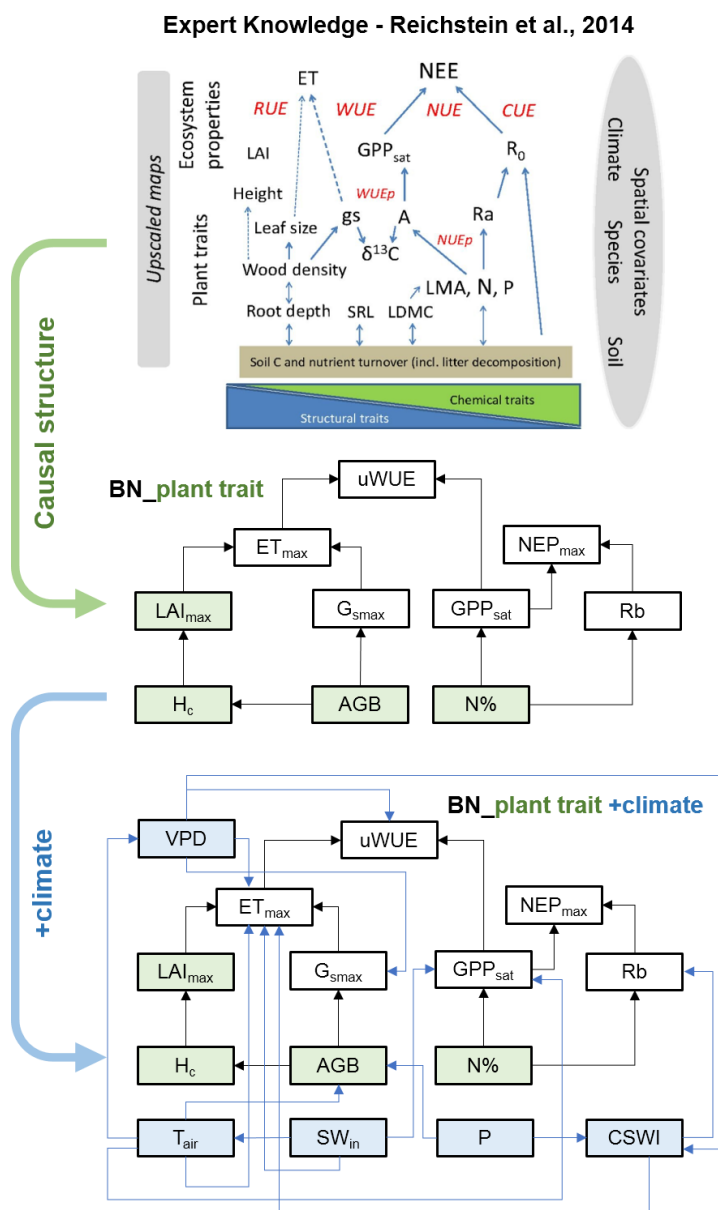
104 **2.2 BN for analyzing causal relations**

105 **2.2.1 BN structures**

106 Based on expert knowledge (Reichstein et al., 2014), we constructed the structure of BN containing the causal
 107 relationships between plant traits and ecosystem function variables: 'BN_plant_trait'. The causal links between
 108 the variables were referred to the relationship diagram in the upper part of Figure 1. Further, we added the

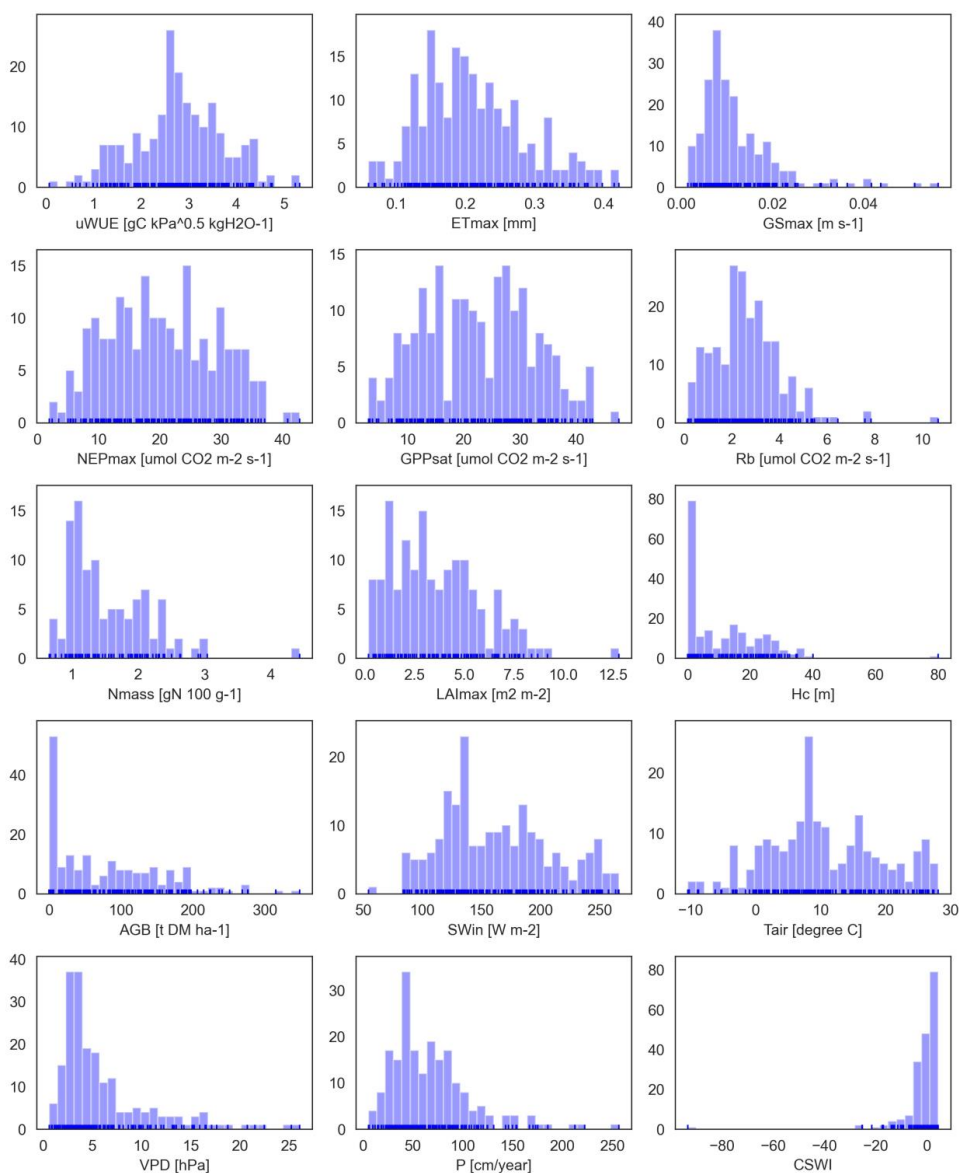


109 climate variables and the corresponding causal relationships, expanding 'BN_plant_trait' to
 110 'BN_plant_trait+climate', which further incorporates the climate variables and their impacts on the system.
 111
 112 Each node is discretized for the BN compiling by the software Netica, while the selection of the thresholds for
 113 classifications (Table 1) is based on the distribution of the values of each node (Figure 2) and also the meanings
 114 of the thresholds. In this step, the three-level discretization (the distribution of a node is divided into three
 115 levels) for each node is applied given the limitation of the amount of training data.
 116





118 Figure 1. The structure of two Bayesian networks (BNs) for attribution of variations in ecosystem functions.
119 BN_pure in the lower left part assumes that all variables of plant traits (box in slight green) and climate (box in
120 slight blue) directly affect the ecosystem function variables (box in white). ‘BN_plant_trait’ in the median part
121 incorporated the causal effects of plant traits (box in slight green) on ecosystem functions (box in white) from
122 expert knowledge as the relation diagram on the upper part (Reichstein et al., 2014). ‘BN_plant_trait+climate’ in
123 the lower part further incorporated the causal impacts of climate variables (box in light blue).



124
125 Figure 2. Distributions of values of ecosystem functions and climate and plant trait variables. The vertical axis
126 indicates the number of flux stations.



127 **2.2.2 Sensitivity analysis based on BN**

128 Based on the Bayesian network (BN), the joint impacts of multiple variables and their causal relations are
129 analyzed. A BN can be represented by nodes X_1, X_2, X_3 to X_n and the joint distribution (Pearl, 1985):

130
$$Pa(X) = Pa(X_1, X_2, \dots, X_n) = \prod_{i=1}^n Pa(X_i | pa(X_i)) \quad (1)$$

131 where $pa(X_i)$ is the probability of the parent node X_i . Expectation-maximization (Moon, 1996) is used to address
132 the data with missing values and then compile the BN.

133

134 Sensitivity analysis is used for the evaluation of the strength of the causal relations between nodes based on
135 mutual information (MI). MI is calculated as the entropy reduction of the child node resulting from changes
136 found at the parent node (Shi et al., 2020a):

137
$$MI = H(Q) - H(Q|F) = \sum_q \sum_f P(q, f) \log_2 \left(\frac{P(q, f)}{P(q)P(f)} \right) \quad (2)$$

138 where H represents the entropy, Q represents the target node, F represents the set of other nodes and q and f
139 represent the status of Q and F .

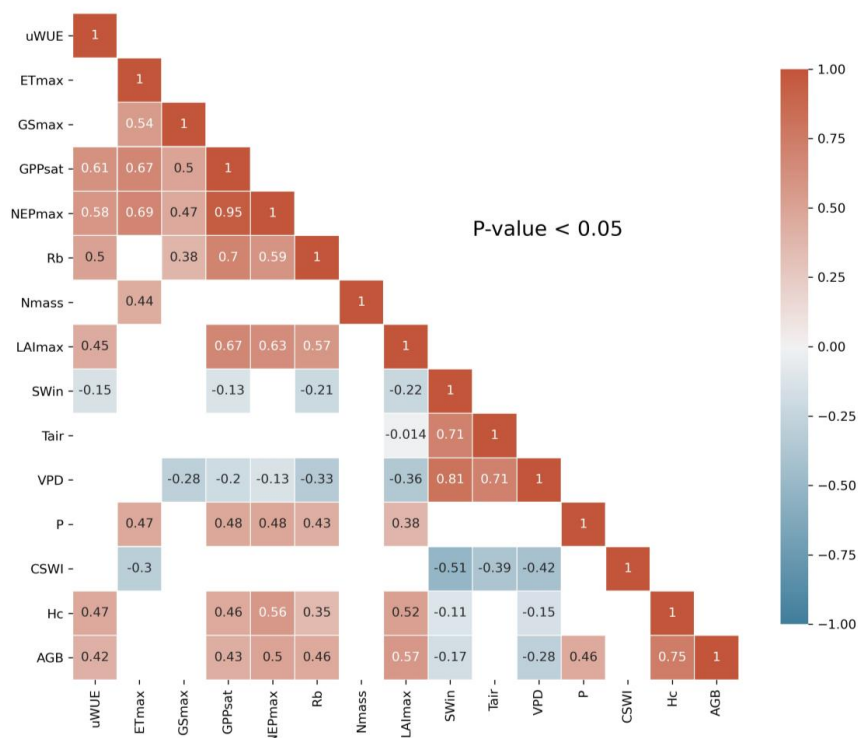
140

141 In this study, we assessed the sensitivity of ecosystem function variables to climate and plant trait variables.
142 Further, to clarify the adding-values of considering causality in the attribution analysis of controls on ecosystem
143 functions, the results of the BN-based sensitivity analysis were compared with the results of additional linear
144 correlation analysis and the previous study using RF (Migliavacca et al., 2021) without considering the causality
145 by comparing the ranking of MI, IMP (the feature importance metric of RF), and Pearson correlation
146 coefficients (the metric of linear correlation analysis) of climate and plant trait variables and their differences in
147 the results of the three methods. Although six ecosystem function variables were directly used in this study, the
148 target variables of the RF-based approach were the first three principal components (PC): PC1, PC2, and PC3
149 (Migliavacca et al., 2021) of the 12 ecosystem variables (including the six variables selected in this study), the
150 connotations of the target variables were relatively consistent between them.

151 **3 Results**

152 **3.1 Correlation analysis**

153 Linear correlation analysis of the variables (Figure 3) showed significant ($P < 0.05$) linear correlations between
154 the ecosystem function variables and some of the climate and plant trait variables. SWin, VPD, and showed
155 negative correlations with these ecosystem function variables. In addition, the majority of the ecosystem
156 function variables showed significant ($P < 0.05$) positive correlations with each other.



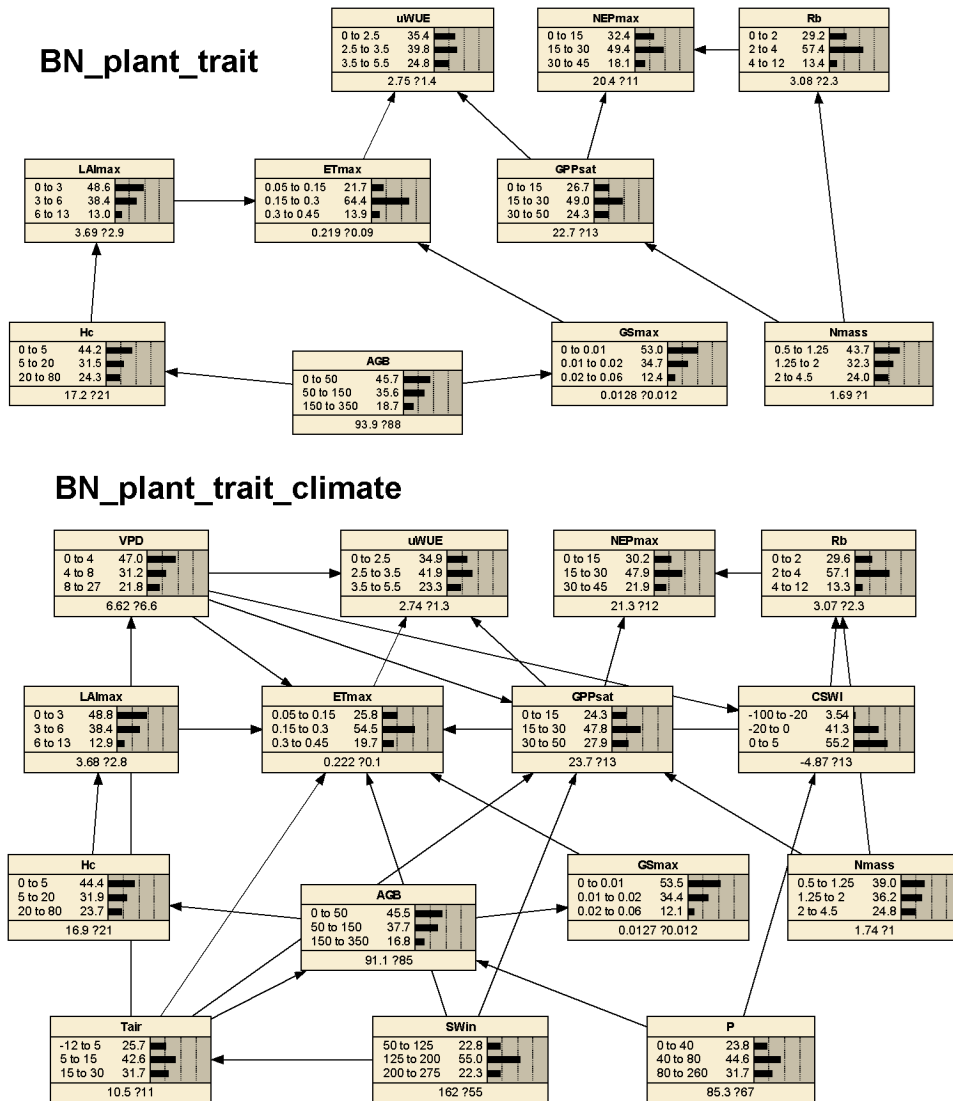
157

158 Figure 3. Correlation coefficient matrix of ecosystem service functions and climate and plant trait variables for
 159 FLUXNET sites. Only correlation coefficients with p-values less than 0.05 level of significance are shown.

160 **3.2 BN-based analysis**

161 We compiled two different BNs (i.e., BN_plant_trait and BN_plant_trait_climate) (Figure 4) and found that the
 162 probability distributions of the values of the common nodes (ecosystem function and plant trait variable nodes)
 163 differed little between the two BNs. This indicates that the compilation was successful and that the inclusion of
 164 climate variables in BN_plant_trait_climate did not alter the fit of the local networks of ecosystem function and
 165 plant trait variables of BN_plant_trait.

166



167

168

169

170

171

172

173

174

175

176

Figure 4. The compiled two BNs ('BN_plant_trait' and 'BN_plant_trait_climate'). The bars of each node represent its probability distribution. At the bottom part of each node, the left and right side values of the '?' are the mean and standard deviation of the distribution, respectively.

We performed sensitivity analyses (Figure 5) on the ecosystem function variables in both BNs to assess their sensitivity to various climate and plant trait variables. We also calculated the difference in sensitivity MI between the two BNs (Figure 5) to compare the change in sensitivity of ecosystem function to each variable after adding further climate variables to the plant trait variables only.



177 The sensitivity of different ecosystem function variables to plant traits and climate variables was highly variable
178 in both BNs (except for the similar pattern between GPPsat and NEPmax). The magnitude of sensitivity of
179 ecosystem functional nodes to plant traits and climate variables was related to whether these plant traits and
180 climate variables were set as their parent nodes. In BN_plant_trait, for the carbon fluxes GPPsat and NEPmax,
181 Nmass had a higher sensitivity due to Nmass being set as their parent node. For the water flux ETmax, it does
182 not have high sensitivity to plant trait variables such as LAImax, Hc, and AGB, although these plant trait
183 variables are set as the parent nodes of ETmax. This indicates the difference in the strength of the control effects
184 of plant traits on carbon and water fluxes.

185

186 In the sensitivity analysis of BN_plant_trait_climate, the sensitivity patterns of the ecosystem function variables
187 changed as a result of the inclusion of climate variables and the change in causality they introduced. The
188 sensitivity of the ecosystem function variables (except GSmax and Rb) to climate variables was significantly
189 increased (especially for Tair and VPD). Their sensitivity to plant trait variables (e.g., Nmass and LAImax)
190 decreased. Among the controls for ETmax and uWUE, climate variables showed a role beyond plant traits,
191 while among the controls for GPPsat and NEPmax, the climate variable Tair also showed a significant role at a
192 similar level to Nmass. The control of plant traits on ecosystem function in BN_plant_trait is also partially
193 transformed into an indirect effect of climate variables by first controlling plant trait variables and then
194 controlling ecosystem function. For example, in BN_plant_trait_climate, for ETmax, a decrease in the
195 sensitivity of ETmax to LAImax and an increase in the sensitivity to Tair was observed after the loop of Tair
196 controlling LAImax and then ETmax was set. This can be explained by the fact that higher temperatures
197 promote vegetation growth and thus may increase LAImax, which then indirectly contributes to the increase in
198 ETmax. In previous studies based on statistical methods that did not consider the systematic causality, this
199 indirect control on ETmax from Tair may have been included in the contribution of LAImax to ETmax.



200

201

202

203

204

205

206

207

208

Figure 5. Sensitivity of ecosystem function variables to other variables in different networks based on mutual information (MI). The left column is the sensitivity analysis of BN_plant_trait, the middle column is the sensitivity analysis of BN_plant_trait_climate, and the right column is the difference between the reported sensitivity of BN_plant_trait_climate and the sensitivity of BN_plant_trait. For BN_plant_trait, the MI values of climate variables to ecosystem function variables are all 0 because they do not contain climate variables. For each ecosystem function in these two BNs, its sensitivity to its child node is not shown (set as 0) because child nodes are not considered causal variables and thus are not evaluated in the attribution.



209 **3.3 Comparing results from RF-based, BN-based analysis, and correlation analysis**

210 To compare the differences between cause-based and non-cause-based attribution or contribution analyses, we
 211 compared the importance ranking of variables based on the RF-based IMP in the study of Migliavacca et al., the
 212 absolute values of the correlation coefficients from the correlation analysis in this study, and the values of MI
 213 from the BN-based sensitivity analysis.

214
 215 Since plant traits such as LAImax, Hc, and AGB were not set as parent nodes of carbon fluxes such as NEPmax
 216 and GPPsat in BN in this study, the effects of LAImax, Hc, and AGB on carbon flux-related variables in
 217 ecosystem function were weaker in the BN-based sensitivity analysis than in the RF-based and correlation
 218 analyses. However, AGB did not show a significant linear correlation with GSmax in the correlation analysis,
 219 suggesting that its control effect on GSmax may be nonlinear but detected by both RF and BN-based attribution
 220 analyses. Of the meteorological variables, Tair showed stronger control over ecosystem function variables in the
 221 BN-based attribution (compared to other climate and plant trait variables), implying that the RF-based
 222 imputation of IMP may have underestimated the role of Tair.

	Methods	Nmass	LAImax	Hc	AGB	SWin	Tair	VPD	P	CSWI
PC1	RF_imp	10.80%	16.60%	14.50%	15.50%	7.60%	9.10%	11.70%	6.70%	4.00%
PC2	RF_imp	5.10%	4.50%	14.90%	5.10%	10.70%	11.20%	7.40%	9.00%	8.30%
PC3	RF_imp	7.00%	2.80%	5.40%	10.70%	9.30%	8.00%	15.40%	6.50%	4.90%
uWUE	BN_sens	0.010	0.000	0.000	0.001	0.011	0.027	0.038	0.000	0.011
ETmax	BN_sens	0.000	0.008	0.005	0.014	0.051	0.077	0.054	0.001	0.040
GSmax	BN_sens	0.000	0.002	0.008	0.037	0.000	0.003	0.000	0.003	0.000
NEPmax	BN_sens	0.049	0.000	0.000	0.005	0.012	0.053	0.019	0.000	0.001
GPPsat	BN_sens	0.082	0.000	0.000	0.007	0.019	0.068	0.033	0.000	0.002
Rb	BN_sens	0.046	0.000	0.000	0.000	0.000	0.001	0.002	0.000	0.005
uWUE	linear_corr		0.45	0.47	0.42	0.15				
ETmax	linear_corr	0.44							0.47	0.30
GSmax	linear_corr							0.28		
NEPmax	linear_corr		0.63	0.56	0.50			0.13	0.48	
GPPsat	linear_corr		0.67	0.46	0.43	0.13		0.20	0.48	
Rb	linear_corr		0.57	0.35	0.46	0.21		0.33	0.43	

223
 224 Figure 6. Comparisons of relationships of ecosystem functional variables to plant traits and climate variables in
 225 different analyses. Method RF_imp is Random forest variable importance (Migliavacca et al., 2021). Method
 226 linear_corr is Linear correlation analysis with the absolute values of Pearson correlation coefficients. Method
 227 BN_sens is a BN-based sensitivity analysis with sensitivity values MI reported. PC1, PC2, and PC3 are the first
 228 three major axes of ecosystem function reported in the study by Migliavacca et al. (Migliavacca et al., 2021)
 229 obtained from principal component analysis of 12 ecosystem function variables which including the six
 230 variables uWUE, ETmax, GSmax, NEPmax, GPPsat, and Rb used in this study (Method BN_sens and
 231 linear_corr in the lower part). The first axis (PC1) explains 39.3% of the variance and is dominated by
 232 maximum ecosystem productivity properties, as indicated by the loadings of GPPsat and NEPmax, and
 233 maximum evapotranspiration (ETmax). The second axis (PC2) explains 21.4% of the variance and refers to
 234 water-use strategies as shown by the loadings of water-use efficiency metrics, evaporative fraction, and GSmax.
 235 The third axis (PC3) explains 11.1% of the variance and includes key attributes that reflect the carbon-use
 236 efficiency of ecosystems. PC3 is dominated by apparent carbon-use efficiency, basal ecosystem respiration



237 (Rb), and the amplitude of evaporative fraction (Migliavacca et al., 2021). The values in each row are in red for
238 high values and in blue for low values, for rows with very few values, the color-based indication is not reliable
239 in ranking the control effects of plant traits and climate variables.

240 **4 Discussions**

241 Previous studies of ‘climate-plant trait-ecosystem function’ relationships have predominantly used only non-
242 causal statistical methods such as RF (Migliavacca et al., 2021). Based on BN, this study investigates the
243 prospect of using causal networks to revisit and attribute the control of climate and plant trait changes to
244 ecosystem function. Compared to traditional correlation analysis and machine learning methods, BN can
245 uncover the effects of causal relationships between variables. This causality discovery can improve on previous
246 findings for studies of ecosystem-climate interactions.

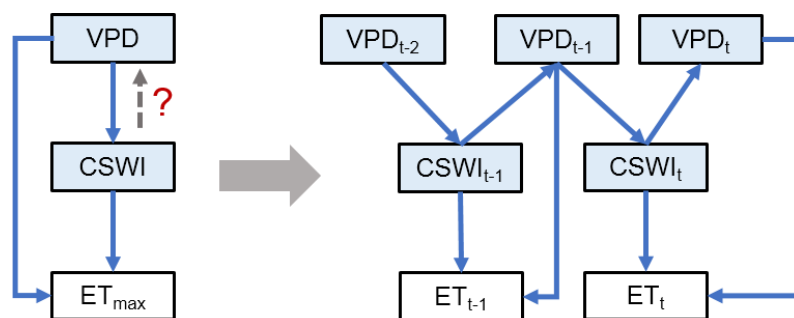
247
248 Because of the inclusion of the constraints provided by expert knowledge (Reichstein et al., 2014), BN-based
249 attribution analysis is relatively reliable and can update our knowledge of the contribution of some
250 teleconnection variables through causal chains. However, since the structure of the expert knowledge graph did
251 not connect LAImax, Hc, and AGB to GPP (Figure 1), LAImax, Hc, and AGB are not set as parent nodes of
252 GPPsat in our BN, and thus the sensitivity of carbon fluxes to LAImax, Hc, AGB, etc. is 0 or close to 0.
253 Therefore, in our BN, the causal controls of LAImax, Hc, and AGB on GPPsat are not shown although they are
254 commonly thought to strongly influence GPPsat and NEPmax. This also demonstrates from another perspective
255 the importance of a reasonable parent node in the attribution analysis using BN, where if a variable cannot be
256 connected to the target variable through a causal loop, the sensitivity of the target variable to it may be low, and
257 this will therefore affect the assessment of the strength of causality. If we want to explicitly measure the
258 response of the target variable to the causality of a variable, it is indeed necessary to set up a causal link between
259 them in BN.

260
261 In this study, it was found that the indirect impacts of some meteorological variables such as Tair may be
262 underestimated in the attribution of ecosystem function when using a non-causal approach. This suggests the
263 feasibility of quantifying indirect causal effects among various variables to help us gain a more systematic
264 understanding. The effective implementation of BN-based causal analysis may depend on the reliability of the
265 causal relationships provided by expert knowledge (directional links between variables). We can establish the
266 connection relationships and network structures between variables from expert knowledge and assign the
267 specific quantification of the connection relationships (conditional probability tables) to the observations and
268 data (Shi et al., 2021a). In the future, we can revisit the linkages of ecosystem functions with climate and
269 environmental systems using BN-based causal analysis to understand the strength and mechanisms of the
270 relationships between direct, indirect, and remotely related effects of variables. Such a data-driven causal
271 analysis framework provides more structured information about climate, plant traits, and ecosystem systems,
272 thus making the data-driven approach more transparent and interpretable (compared to previous black-box
273 models (Rudin, 2019)). If further combined with findings from process-based models, it is promising to
274 significantly improve our understanding of the complex ‘climate-plant trait-ecosystem function’ relationships by
275 comparing detailed relationships and structural influences between variables.



276
277 Besides, the BN in this study was mainly based on data averaged over multiple years, thus possibly partially
278 underestimating the effect of temporal variations in the relationships between variables. Another limitation of
279 the BN proposed above is that the causal relationships between variables are unidirectional, while it is difficult
280 to represent interactions and feedback between variables (Marcot and Penman, 2019). In future studies, to
281 address these two issues, BN based on temporal dynamics can be promising (Figure 7). By refining the
282 interaction of temporal lags between variables, it is possible to incorporate not only temporal variation but also
283 control factors that attribute interactions and feedback between variables. For example, the interaction and
284 feedback mechanisms of VPD, soil moisture, and ET with lag effects (Figure 7) and their impacts on ecosystems
285 have attracted extensive interest from researchers (Anderegg et al., 2019; Humphrey et al., 2021; Lansu et al.,
286 2020; Liu et al., 2020; Xu et al., 2022; Zhou et al., 2019), but conventional statistical methods have been
287 ineffective in analyzing such relationships with both interactive causality and temporal lags. In contrast, the BN
288 proposed here, which incorporates feedback effects and lagged effects that were common in climate-ecosystem
289 relations (Lin et al., 2019), is potentially able to address this issue from a data-driven approach. When further
290 combined with the findings of process-based models, our understanding of climate and ecosystem interactions
291 and feedback and their mechanisms in time is hopefully deepened.

292



293

294 Figure 7. The future BNs with the temporal causality further considered addressing the causality of the
295 interaction between variables. The VPD-CSWI-ET relationship is used here as an example. t , $t-1$, and $t-2$ denote
296 the current period, the last period, and the period before the last period, respectively. The network on the left
297 only considers the effect of VPD on CSWI without considering the feedback of CSWI on the VPD. The network
298 on the right characterizes the VPD-CSWI interaction with the feedback from CSWI at period $t-1$ to VPD at
299 period t .

300 5 Conclusion

301 By emphasizing causality, based on BN, we revisited and attributed the contribution of climate and plant traits
302 to global terrestrial ecosystem function. The major conclusions of this study include:

- 303 1. BN can be used for the quantification of causal relationships between complex ecosystems and climatic
304 and environmental systems and enables the analysis of indirect effects among variables.



- 305 2. The control of ecosystem function by climate variables (especially Tair and VPD) may have been
306 underestimated in the past, and the mechanism of indirect effects of climate variables on ecosystem
307 function through plant traits should be emphasized in future studies.
- 308 3. Further inclusion of temporal information in BN holds promise for improving the analysis of lagged effects
309 and interactions and feedback effects between variables.
- 310
- 311



312 **Financial support**

313 This research was supported by the National Natural Science Foundation of China (Grant No. U1803243), the
314 Key projects of the Natural Science Foundation of Xinjiang Autonomous Region (Grant No. 2022D01D01), the
315 Strategic Priority Research Program of the Chinese Academy of Sciences (Grant No. XDA20060302), and
316 High-End Foreign Experts Project.

317 **Author Contributions**

318 HS and GL initiated this research and were responsible for the integrity of the work as a whole. HS performed
319 formal analysis and calculations and drafted the manuscript. HS were responsible for the data collection and
320 analysis. GL, PDM, TVdV, OH, and AK contributed resources and financial support.

321 **Competing interests**

322 The authors declare that they have no conflict of interest.

323 **Code availability**

324 The codes that were used for all analyses are available from the first author (shihaiyang16@mailsucas.ac.cn)
325 upon request.

326 **Data availability**

327 The data used in this study can be accessed by contacting the first author (shihaiyang16@mailsucas.ac.cn) upon
328 request.

329

330

331



332 **References**

333 Anderegg, W. R., Trugman, A. T., Bowling, D. R., Salvucci, G., and Tuttle, S. E.: Plant functional
334 traits and climate influence drought intensification and land–atmosphere feedbacks, *Proceedings of*
335 *the National Academy of Sciences*, 116, 14071–14076, 2019.

336 Baldocchi, D.: Measuring fluxes of trace gases and energy between ecosystems and the atmosphere–
337 the state and future of the eddy covariance method, *Global change biology*, 20, 3600–3609, 2014.

338 Barnes, M. L., Farella, M. M., Scott, R. L., Moore, D. J. P., Ponce-Campos, G. E., Biederman, J. A.,
339 MacBean, N., Litvak, M. E., and Breshears, D. D.: Improved dryland carbon flux predictions with
340 explicit consideration of water-carbon coupling, *Commun Earth Environ*, 2, 1–9,
341 <https://doi.org/10.1038/s43247-021-00308-2>, 2021.

342 Chan, T., Ross, H., Hoverman, S., and Powell, B.: Participatory development of a Bayesian network
343 model for catchment-based water resource management, *Water Resour. Res.*, 46,
344 <https://doi.org/10.1029/2009WR008848>, 2010.

345 Diaz, S. and Cabido, M.: Plant functional types and ecosystem function in relation to global change,
346 *Journal of Vegetation Science*, 8, 463–474, <https://doi.org/10.2307/3237198>, 1997.

347 Flechard, C. R., Ibrom, A., Skiba, U. M., de Vries, W., van Oijen, M., Cameron, D. R., Dise, N. B.,
348 Korhonen, J. F. J., Buchmann, N., Legout, A., Simpson, D., Sanz, M. J., Aubinet, M., Loustau, D.,
349 Montagnani, L., Neirynek, J., Janssens, I. A., Pihlatie, M., Kiese, R., Siemens, J., Francez, A.-J.,
350 Augustin, J., Varlagin, A., Olejnik, J., Juszczak, R., Aurela, M., Berveiller, D., Chojnicki, B. H.,
351 Dämmgen, U., Delpierre, N., Djuricic, V., Drewer, J., Dufrêne, E., Eugster, W., Fauvel, Y., Fowler,
352 D., Frumau, A., Granier, A., Gross, P., Hamon, Y., Helfter, C., Hensen, A., Horváth, L., Kitzler, B.,
353 Kruijt, B., Kutsch, W. L., Lobo-do-Vale, R., Lohila, A., Longdoz, B., Marek, M. V., Matteucci, G.,
354 Mitisinkova, M., Moreaux, V., Neftel, A., Ourcival, J.-M., Pilegaard, K., Pita, G., Sanz, F.,
355 Schjoerring, J. K., Sebastià, M.-T., Tang, Y. S., Uggerud, H., Urbaniak, M., van Dijk, N., Vesala, T.,
356 Vidic, S., Vincke, C., Weidinger, T., Zechmeister-Boltenstern, S., Butterbach-Bahl, K., Nemitz, E.,
357 and Sutton, M. A.: Carbon–nitrogen interactions in European forests and semi-natural vegetation –
358 Part 1: Fluxes and budgets of carbon, nitrogen and greenhouse gases from ecosystem monitoring and
359 modelling, *Biogeosciences*, 17, 1583–1620, <https://doi.org/10.5194/bg-17-1583-2020>, 2020.

360 Fleischer, K., Wårlind, D., Van der Molen, M. K., Rebel, K. T., Arneth, A., Erisman, J. W., Wassen,
361 M. J., Smith, B., Gough, C. M., and Margolis, H. A.: Low historical nitrogen deposition effect on
362 carbon sequestration in the boreal zone, *Journal of Geophysical Research: Biogeosciences*, 120,
363 2542–2561, 2015.

364 Friedman, N., Geiger, D., and Goldszmidt, M.: Bayesian network classifiers, *Machine learning*, 29,
365 131–163, 1997.

366 Gregorutti, B., Michel, B., and Saint-Pierre, P.: Correlation and variable importance in random
367 forests, *Statistics and Computing*, 27, 659–678, 2017.

368 Grimm, N. B., Chapin III, F. S., Bierwagen, B., Gonzalez, P., Groffman, P. M., Luo, Y., Melton, F.,
369 Nadelhoffer, K., Pairis, A., and Raymond, P. A.: The impacts of climate change on ecosystem
370 structure and function, *Frontiers in Ecology and the Environment*, 11, 474–482, 2013.

371 Humphrey, V., Berg, A., Ciais, P., Gentine, P., Jung, M., Reichstein, M., Seneviratne, S. I., and
372 Frankenberg, C.: Soil moisture–atmosphere feedback dominates land carbon uptake variability,
373 *Nature*, 592, 65–69, <https://doi.org/10.1038/s41586-021-03325-5>, 2021.



- 374 Jung, M., Reichstein, M., Ciais, P., Seneviratne, S. I., Sheffield, J., Goulden, M. L., Bonan, G.,
375 Cescatti, A., Chen, J., de Jeu, R., Dolman, A. J., Eugster, W., Gerten, D., Gianelle, D., Gobron, N.,
376 Heinke, J., Kimball, J., Law, B. E., Montagnani, L., Mu, Q., Mueller, B., Oleson, K., Papale, D.,
377 Richardson, A. D., Rouspard, O., Running, S., Tomelleri, E., Viovy, N., Weber, U., Williams, C.,
378 Wood, E., Zaehle, S., and Zhang, K.: Recent decline in the global land evapotranspiration trend due to
379 limited moisture supply, *Nature*, 467, 951–954, <https://doi.org/10.1038/nature09396>, 2010.
- 380 Jung, M., Schwalm, C., Migliavacca, M., Walther, S., Camps-Valls, G., Koirala, S., Anthoni, P.,
381 Besnard, S., Bodesheim, P., Carvalhais, N., Chevallier, F., Gans, F., S Goll, D., Haverd, V., Köhler,
382 P., Ichii, K., K Jain, A., Liu, J., Lombardozi, D., E M S Nabel, J., A Nelson, J., O’Sullivan, M.,
383 Pallandt, M., Papale, D., Peters, W., Pongratz, J., Rödenbeck, C., Sitch, S., Tramontana, G., Walker,
384 A., Weber, U., and Reichstein, M.: Scaling carbon fluxes from eddy covariance sites to globe:
385 Synthesis and evaluation of the FLUXCOM approach, *Biogeosciences*, 17, 1343–1365,
386 <https://doi.org/10.5194/bg-17-1343-2020>, 2020.
- 387 Keshtkar, A. R., Salajegheh, A., Sadoddin, A., and Allan, M. G.: Application of Bayesian networks
388 for sustainability assessment in catchment modeling and management (Case study: The Hablehood
389 river catchment), *Ecological Modelling*, 268, 48–54, 2013.
- 390 Lansu, E. M., van Heerwaarden, C., Stegehuis, A. I., and Teuling, A. J.: Atmospheric aridity and
391 apparent soil moisture drought in European forest during heat waves, *Geophysical Research Letters*,
392 47, e2020GL087091, 2020.
- 393 Lin, C., Gentine, P., Frankenberg, C., Zhou, S., Kennedy, D., and Li, X.: Evaluation and mechanism
394 exploration of the diurnal hysteresis of ecosystem fluxes, *Agricultural and Forest Meteorology*, 278,
395 107642, <https://doi.org/10.1016/j.agrformet.2019.107642>, 2019.
- 396 Liu, L., Gudmundsson, L., Hauser, M., Qin, D., Li, S., and Seneviratne, S. I.: Soil moisture dominates
397 dryness stress on ecosystem production globally, *Nature communications*, 11, 1–9, 2020.
- 398 Madani, N., Kimball, J. S., Ballantyne, A. P., Affleck, D. L. R., van Bodegom, P. M., Reich, P. B.,
399 Kattge, J., Sala, A., Nazeri, M., Jones, M. O., Zhao, M., and Running, S. W.: Future global
400 productivity will be affected by plant trait response to climate, *Sci Rep*, 8, 2870,
401 <https://doi.org/10.1038/s41598-018-21172-9>, 2018.
- 402 Manning, P., Van Der Plas, F., Soliveres, S., Allan, E., Maestre, F. T., Mace, G., Whittingham, M. J.,
403 and Fischer, M.: Redefining ecosystem multifunctionality, *Nature ecology & evolution*, 2, 427–436,
404 2018.
- 405 Marcot, B. G. and Penman, T. D.: Advances in Bayesian network modelling: Integration of modelling
406 technologies, *Environmental modelling & software*, 111, 386–393, 2019.
- 407 Migliavacca, M., Reichstein, M., Richardson, A. D., Colombo, R., Sutton, M. A., Lasslop, G.,
408 Tomelleri, E., Wohlfahrt, G., Carvalhais, N., and Cescatti, A.: Semiempirical modeling of abiotic and
409 biotic factors controlling ecosystem respiration across eddy covariance sites, *Global Change Biology*,
410 17, 390–409, 2011.
- 411 Migliavacca, M., Musavi, T., Mahecha, M. D., Nelson, J. A., Knauer, J., Baldocchi, D. D., Perez-
412 Priego, O., Christiansen, R., Peters, J., Anderson, K., Bahn, M., Black, T. A., Blanken, P. D., Bonal,
413 D., Buchmann, N., Caldararu, S., Carrara, A., Carvalhais, N., Cescatti, A., Chen, J., Cleverly, J.,
414 Cremonese, E., Desai, A. R., El-Madany, T. S., Farella, M. M., Fernández-Martínez, M., Filippa, G.,
415 Forkel, M., Galvagno, M., Gomasasca, U., Gough, C. M., Göckede, M., Ibrom, A., Ikawa, H.,
416 Janssens, I. A., Jung, M., Kattge, J., Keenan, T. F., Knohl, A., Kobayashi, H., Kraemer, G., Law, B.
417 E., Liddell, M. J., Ma, X., Mammarella, I., Martini, D., Macfarlane, C., Matteucci, G., Montagnani,
418 L., Pabon-Moreno, D. E., Panigada, C., Papale, D., Pendall, E., Penuelas, J., Phillips, R. P., Reich, P.



- 419 B., Rossini, M., Rotenberg, E., Scott, R. L., Stahl, C., Weber, U., Wohlfahrt, G., Wolf, S., Wright, I.
420 J., Yakir, D., Zaehle, S., and Reichstein, M.: The three major axes of terrestrial ecosystem function,
421 *Nature*, 598, 468–472, <https://doi.org/10.1038/s41586-021-03939-9>, 2021.
- 422 Milns, I., Beale, C. M., and Smith, V. A.: Revealing ecological networks using Bayesian network
423 inference algorithms, *Ecology*, 91, 1892–1899, <https://doi.org/10.1890/09-0731.1>, 2010.
- 424 Moon, T. K.: The expectation-maximization algorithm, *IEEE Signal processing magazine*, 13, 47–60,
425 1996.
- 426 Musavi, T., Mahecha, M. D., Migliavacca, M., Reichstein, M., van de Weg, M. J., van Bodegom, P.
427 M., Bahn, M., Wirth, C., Reich, P. B., and Schrod, F.: The imprint of plants on ecosystem
428 functioning: A data-driven approach, *International Journal of Applied Earth Observation and*
429 *Geoinformation*, 43, 119–131, 2015.
- 430 Musavi, T., Migliavacca, M., van de Weg, M. J., Kattge, J., Wohlfahrt, G., van Bodegom, P. M.,
431 Reichstein, M., Bahn, M., Carrara, A., and Domingues, T. F.: Potential and limitations of inferring
432 ecosystem photosynthetic capacity from leaf functional traits, *Ecology and evolution*, 6, 7352–7366,
433 2016.
- 434 Myers-Smith, I. H., Thomas, H. J. D., and Bjorkman, A. D.: Plant traits inform predictions of tundra
435 responses to global change, *New Phytologist*, 221, 1742–1748, <https://doi.org/10.1111/nph.15592>,
436 2019.
- 437 Nelson, J. A., Carvalhais, N., Migliavacca, M., Reichstein, M., and Jung, M.: Water-stress-induced
438 breakdown of carbon–water relations: indicators from diurnal FLUXNET patterns, *Biogeosciences*,
439 15, 2433–2447, 2018.
- 440 Pastorello, G., Trotta, C., Canfora, E., Chu, H., Christianson, D., Cheah, Y.-W., Poindexter, C., Chen,
441 J., Elbashandy, A., Humphrey, M., Isaac, P., Polidori, D., Reichstein, M., Ribeca, A., van Ingen, C.,
442 Vuichard, N., Zhang, L., Amiro, B., Ammann, C., Arain, M. A., Ardö, J., Arkebauer, T., Arndt, S. K.,
443 Arriga, N., Aubinet, M., Aurela, M., Baldocchi, D., Barr, A., Beamesderfer, E., Marchesini, L. B.,
444 Bergeron, O., Beringer, J., Bernhofer, C., Berveiller, D., Billesbach, D., Black, T. A., Blanken, P. D.,
445 Bohrer, G., Boike, J., Bolstad, P. V., Bonal, D., Bonnefond, J.-M., Bowling, D. R., Bracho, R.,
446 Brodeur, J., Brümmer, C., Buchmann, N., Burban, B., Burns, S. P., Buysse, P., Cale, P., Cavagna, M.,
447 Cellier, P., Chen, S., Chini, I., Christensen, T. R., Cleverly, J., Collalti, A., Consalvo, C., Cook, B. D.,
448 Cook, D., Coursolle, C., Cremonese, E., Curtis, P. S., D’Andrea, E., da Rocha, H., Dai, X., Davis, K.
449 J., Cinti, B. D., Grandcourt, A. de, Ligne, A. D., De Oliveira, R. C., Delpierre, N., Desai, A. R., Di
450 Bella, C. M., Tommasi, P. di, Dolman, H., Domingo, F., Dong, G., Dore, S., Duce, P., Dufrêne, E.,
451 Dunn, A., Dušek, J., Eamus, D., Eichelmann, U., ElKhidir, H. A. M., Eugster, W., Ewenz, C. M.,
452 Ewers, B., Famulari, D., Fares, S., Feigenwinter, I., Feitz, A., Fensholt, R., Filippa, G., Fischer, M.,
453 Frank, J., Galvagno, M., et al.: The FLUXNET2015 dataset and the ONEFlux processing pipeline for
454 eddy covariance data, *Sci Data*, 7, 225, <https://doi.org/10.1038/s41597-020-0534-3>, 2020.
- 455 Pearl, J.: Bayesian networks: A model of self-activated memory for evidential reasoning, in:
456 *Proceedings of the 7th Conference of the Cognitive Science Society*, University of California, Irvine,
457 CA, USA, 15–17, 1985.
- 458 Peaucelle, M., Bacour, C., Ciais, P., Vuichard, N., Kuppel, S., Peñuelas, J., Beletti Marchesini, L.,
459 Blanken, P. D., Buchmann, N., and Chen, J.: Covariations between plant functional traits emerge from
460 constraining parameterization of a terrestrial biosphere model, *Global ecology and biogeography*, 28,
461 1351–1365, 2019.



- 462 Pollino, C. A., Woodberry, O., Nicholson, A., Korb, K., and Hart, B. T.: Parameterisation and
463 evaluation of a Bayesian network for use in an ecological risk assessment, *Environmental Modelling*
464 & Software, 22, 1140–1152, <https://doi.org/10.1016/j.envsoft.2006.03.006>, 2007.
- 465 Reichstein, M., Bahn, M., Mahecha, M. D., Kattge, J., and Baldocchi, D. D.: Linking plant and
466 ecosystem functional biogeography, *Proceedings of the National Academy of Sciences*, 111, 13697–
467 13702, <https://doi.org/10.1073/pnas.1216065111>, 2014.
- 468 Reichstein, M., Camps-Valls, G., Stevens, B., Jung, M., Denzler, J., Carvalhais, N., and Prabhat:
469 Deep learning and process understanding for data-driven Earth system science, *Nature*, 566, 195–204,
470 <https://doi.org/10.1038/s41586-019-0912-1>, 2019.
- 471 Rudin, C.: Stop explaining black box machine learning models for high stakes decisions and use
472 interpretable models instead, *Nat Mach Intell*, 1, 206–215, <https://doi.org/10.1038/s42256-019-0048->
473 [x](https://doi.org/10.1038/s42256-019-0048-x), 2019.
- 474 Sakschewski, B., von Bloh, W., Boit, A., Poorter, L., Peña-Claros, M., Heinke, J., Joshi, J., and
475 Thonicke, K.: Resilience of Amazon forests emerges from plant trait diversity, *Nature Clim Change*,
476 6, 1032–1036, <https://doi.org/10.1038/nclimate3109>, 2016.
- 477 Santoro, M., Cartus, O., Carvalhais, N., Rozendaal, D. M. A., Avitabile, V., Araza, A., de Bruin, S.,
478 Herold, M., Quegan, S., Rodríguez-Veiga, P., Balzter, H., Carreiras, J., Schepaschenko, D., Korets,
479 M., Shimada, M., Itoh, T., Moreno Martínez, Á., Cavlovic, J., Cazzolla Gatti, R., da Conceição Bispo,
480 P., Dewnath, N., Labrière, N., Liang, J., Lindsell, J., Mitchard, E. T. A., Morel, A., Pacheco
481 Pascagaza, A. M., Ryan, C. M., Slik, F., Vaglio Laurin, G., Verbeeck, H., Wijaya, A., and Willcock,
482 S.: The global forest above-ground biomass pool for 2010 estimated from high-resolution satellite
483 observations, *Earth System Science Data*, 13, 3927–3950, <https://doi.org/10.5194/essd-13-3927-2021>,
484 2021.
- 485 Shi, H., Luo, G., Zheng, H., Chen, C., Bai, J., Liu, T., Ochege, F. U., and De Maeyer, P.: Coupling the
486 water-energy-food-ecology nexus into a Bayesian network for water resources analysis and
487 management in the Syr Darya River basin, *Journal of Hydrology*, 581, 124387,
488 <https://doi.org/10.1016/j.jhydrol.2019.124387>, 2020a.
- 489 Shi, H., Luo, G., Zheng, H., Chen, C., Hellwich, O., Bai, J., Liu, T., Liu, S., Xue, J., Cai, P., He, H.,
490 Ochege, F. U., Van de Voorde, T., and de Maeyer, P.: A novel causal structure-based framework for
491 comparing a basin-wide water–energy–food–ecology nexus applied to the data-limited Amu Darya
492 and Syr Darya river basins, *Hydrology and Earth System Sciences*, 25, 901–925,
493 <https://doi.org/10.5194/hess-25-901-2021>, 2021a.
- 494 Shi, H., Pan, Q., Luo, G., Hellwich, O., Chen, C., Voorde, T. V. de, Kurban, A., De Maeyer, P., and
495 Wu, S.: Analysis of the Impacts of Environmental Factors on Rat Hole Density in the Northern Slope
496 of the Tianshan Mountains with Satellite Remote Sensing Data, *Remote Sensing*, 13, 4709,
497 <https://doi.org/10.3390/rs13224709>, 2021b.
- 498 Shi, H., Luo, G., Hellwich, O., Xie, M., Zhang, C., Zhang, Y., Wang, Y., Yuan, X., Ma, X., Zhang,
499 W., Kurban, A., De Maeyer, P., and Van de Voorde, T.: Evaluation of water flux predictive models
500 developed using eddy covariance observations and machine learning: a meta-analysis, *Hydrology and*
501 *Earth System Sciences Discussions*, 1–21, <https://doi.org/10.5194/hess-2022-90>, 2022a.
- 502 Shi, H., Luo, G., Hellwich, O., Xie, M., Zhang, C., Zhang, Y., Wang, Y., Yuan, X., Ma, X., Zhang,
503 W., Kurban, A., De Maeyer, P., and Van de Voorde, T.: Variability and uncertainty in flux-site-scale
504 net ecosystem exchange simulations based on machine learning and remote sensing: a systematic
505 evaluation, *Biogeosciences*, 19, 3739–3756, <https://doi.org/10.5194/bg-19-3739-2022>, 2022b.



- 506 Shi, Y., Jin, N., Ma, X., Wu, B., He, Q., Yue, C., and Yu, Q.: Attribution of climate and human
507 activities to vegetation change in China using machine learning techniques, *Agricultural and Forest*
508 *Meteorology*, 294, 108146, <https://doi.org/10.1016/j.agrformet.2020.108146>, 2020b.
- 509 Tramontana, G., Jung, M., Schwalm, C. R., Ichii, K., Camps-Valls, G., Ráduly, B., Reichstein, M.,
510 Arain, M. A., Cescatti, A., Kiely, G., Merbold, L., Serrano-Ortiz, P., Sickert, S., Wolf, S., and Papale,
511 D.: Predicting carbon dioxide and energy fluxes across global FLUXNET sites with regression
512 algorithms, *Biogeosciences*, 13, 4291–4313, <https://doi.org/10.5194/bg-13-4291-2016>, 2016.
- 513 Trifonova, N., Kenny, A., Maxwell, D., Duplisea, D., Fernandes, J., and Tucker, A.: Spatio-temporal
514 Bayesian network models with latent variables for revealing trophic dynamics and functional
515 networks in fisheries ecology, *Ecological Informatics*, 30, 142–158,
516 <https://doi.org/10.1016/j.ecoinf.2015.10.003>, 2015.
- 517 Wang, Z., Zhu, D., Wang, X., Zhang, Y., and Peng, S.: Regressions underestimate the direct effect of
518 soil moisture on land carbon sink variability, *Global Change Biology*,
519 <https://doi.org/10.1111/gcb.16422>, 2022.
- 520 Xu, S., McVicar, T. R., Li, L., Yu, Z., Jiang, P., Zhang, Y., Ban, Z., Xing, W., Dong, N., Zhang, H.,
521 and Zhang, M.: Globally assessing the hysteresis between sub-diurnal actual evaporation and vapor
522 pressure deficit at the ecosystem scale: Patterns and mechanisms, *Agricultural and Forest*
523 *Meteorology*, 323, 109085, <https://doi.org/10.1016/j.agrformet.2022.109085>, 2022.
- 524 Zhou, S., Williams, A. P., Berg, A. M., Cook, B. I., Zhang, Y., Hagemann, S., Lorenz, R.,
525 Seneviratne, S. I., and Gentile, P.: Land–atmosphere feedbacks exacerbate concurrent soil drought
526 and atmospheric aridity, *Proceedings of the National Academy of Sciences*, 116, 18848–18853, 2019.
- 527